



Published in final edited form as:

Science. 2016 November 04; 354(6312): . doi:10.1126/science.aag0839.

Exploring Genetic Suppression Interactions on a Global Scale

Jolanda van Leeuwen^{1,*}, Carles Pons^{2,3,*}, Joseph C. Mellor^{1,4,#}, Takafumi N. Yamaguchi^{1,4,5}, Helena Friesen¹, John Koschwanez⁶, Mojca Mattiazzi Ušaj¹, Maria Pechlaner⁷, Mehmet Takar⁸, Matej Ušaj¹, Benjamin VanderSluis^{2,≈}, Kerry Andrusiak^{1,5}, Pritpal Bansal^{1,4}, Anastasia Baryshnikova⁹, Claire Boone¹, Jessica Cao¹, Atina Cote^{1,4}, Marinella Gebbia^{1,4}, Gene Horecka¹, Ira Horecka¹, Elena Kuzmin^{1,5}, Nicole Legro¹, Wendy Liang¹, Natascha van Lieshout^{1,4,5}, Margaret McNee¹, Bryan-Joseph San Luis¹, Fatemeh Shaeri^{1,4}, Ermira Shuteriqi¹, Song Sun¹, Lu Yang¹, Ji-Young Youn⁴, Michael Yuen¹, Michael Costanzo¹, Anne-Claude Gingras^{4,5}, Patrick Aloy^{3,10}, Chris Oostenbrink⁷, Andrew Murray⁶, Todd R. Graham⁸, Chad L. Myers^{2,‡}, Brenda J. Andrews^{1,5,‡}, Frederick P. Roth^{1,4,5,11,‡}, and Charles Boone^{1,5,‡}

¹Donnelly Centre for Cellular and Biomolecular Research, University of Toronto, 160 College St., Toronto ON, Canada M5S 3E1

²Department of Computer Science and Engineering, University of Minnesota-Twin Cities, 200, Union St., Minneapolis MN, U.S.A. 55455

³Institute for Research in Biomedicine (IRB Barcelona), the Barcelona Institute for Science and Technology, Barcelona, Catalonia, Spain

⁴Lunenfeld-Tanenbaum Research Institute, Mount Sinai Hospital, 600 University Ave., Toronto ON, Canada M5G 1X5

⁵Department of Molecular Genetics, University of Toronto, 160 College St., Toronto ON, Canada M5S 3E1

⁶Department of Molecular and Cellular Biology, Harvard University, 52 Oxford St., Cambridge, MA, U.S.A. 02138

⁷Institute of Molecular Modeling and Simulation, University of Natural Resources and Life Sciences, Muthgasse 18, A-1190 Vienna, Austria

⁸Department of Biological Sciences, Vanderbilt University, 1161 21st Ave South, Nashville TN, U.S.A. 37232

⁹Lewis-Sigler Institute for Integrative Genomics, Princeton University, Princeton NJ, U.S.A., 08544

¹⁰Institució Catalana de Recerca i Estudis Avançats, Barcelona, Catalonia, Spain

[‡]To whom correspondence should be addressed. cmyers@cs.umn.edu (C.L.M.);, brenda.andrews@utoronto.ca (B.J.A.); fritz.roth@utoronto.ca (F.P.R.);, charlie.boone@utoronto.ca (C.B.).

[#]Present address: seqWell Inc., 376 Hale St., Beverly MA, U.S.A. 01915

[≈]Present address: Simons Center for Data Analysis, Simons Foundation, 160 Fifth Ave., New York NY, U.S.A. 10010

*These authors contributed equally to this work.

Supplementary Materials:

Materials and Methods, Tables S1 – S7, Figs. S1 – S7, References (48–62)

¹¹Department of Computer Science, University of Toronto, 160 College St., Toronto ON, Canada, M5S 3E1

Abstract

Genetic suppression occurs when the phenotypic defects caused by a mutation in a particular gene are rescued by a mutation in a second gene. To explore the principles of genetic suppression, we examined both literature-curated and unbiased experimental data, involving systematic genetic mapping and whole-genome sequencing, to generate a large-scale suppression network among yeast genes. Most suppression pairs identified novel relationships among functionally related genes, providing new insights into the functional wiring diagram of the cell. In addition to suppressor mutations, we identified frequent secondary mutations, in a subset of genes, that likely cause a delay in the onset of stationary phase, which appears to promote their enrichment within a propagating population. These findings allow us to formulate and quantify general mechanisms of genetic suppression.

Main Text

Although causative variants have been identified for many Mendelian disorders, challenges remain in understanding how genetic variants combine to generate phenotypes. Significant progress has been made in mapping and interpreting genetic interactions in yeast, using growth rate as a proxy for fitness. High-throughput genetic interaction studies have identified hundreds of thousands of negative and positive interactions, in which the fitness defect of a yeast double mutant is either more or less severe, respectively, than the expected effect of combining the single mutants (Fig. 1A) (1, 2). Importantly, positive interactions indicate that the phenotypic effects associated with detrimental mutations can be masked or overcome, and may explain why certain individuals are healthy despite carrying severe disease-causing mutations (3).

Positive interactions can be further classified by their relative strength, ranging from masking, in which the double mutant fitness is higher than expected but less than or equal to that of the slowest growing single mutant, to suppression, in which the double mutant is healthier than the slowest growing single mutant and possibly has a fitness that is comparable to wild type (Fig. 1A) (1, 4). These classes of positive interactions can represent biologically distinct functional relationships (4, 5). Most positive interactions identified by systematic genetic interaction screens in yeast, based on synthetic genetic array (SGA) analysis with loss-of-function mutations (2, 6), are relatively weak masking interactions (Fig. S1A), such as the positive interactions that occur among genes within the same nonessential complex or pathway (7). By contrast, stronger suppression interactions remain largely unexplored.

Spontaneous suppressor mutations can be selected to overcome the fitness defect associated with a specific mutant allele. Extragenic suppressor mutations encompass two basic classes: 1) informational suppressors that change the protein translational or mRNA transcriptional machinery, such that the primary mutation is reinterpreted; and 2) functional suppressors in which a mutation in a second gene functionally compensates for the defect associated with

the primary mutation (8). Here, our major goal was to investigate the general principles of functional suppression by assembling a global network of these interactions, which should provide new mechanistic insights about protein function and enable the ordering of components of biological pathways.

A network of literature-curated suppression interactions

To capture existing suppression interactions in *Saccharomyces cerevisiae*, we examined ~6000 potential interactions in ~1700 published papers derived from the BioGRID's "synthetic rescue" dataset (9). From each interaction, we annotated the type of suppressor mutation (e.g. spontaneous mutation or deletion allele), the type of mutation that is being suppressed, which we refer to as "query" mutation, and the use of specific conditions (e.g. a drug or specialized carbon source). Suppression interactions that were intragenic, involved a specific phenotype other than growth, or included more than two genes, were excluded from the final dataset. We also removed suppression interactions derived from high-throughput experiments or dosage interactions in which either the query or the suppressor was overexpressed. The resulting literature-curated network encompassed 1304 genes and 1842 unique suppression interactions (Table S1). We visualized this network using a force-directed layout (10), so that query genes that share a common suppressor tend to be positioned together (Fig. 1B). Most query genes (69%) are suppressed by one or two suppressor genes, while a small subset of queries (5%) have numerous (10–27) reported interactions (Fig. S1B). Despite the relatively low average network degree, genes involved in highly studied processes, such as DNA replication and repair or chromatin and transcription, tend to group together due to their shared suppression interactions (Fig. 1B).

Combining data from multiple studies can reveal suppression mechanisms between pathways or protein complexes that may not be apparent from any individual study. Indeed, a sub-network focused on DNA replication and repair pathways showed that many of the interactions appear to represent the activation of alternative DNA repair pathways (Fig. 1C). For example, mutations that perturb Rad51-dependent homologous recombination (HR) often lead to toxic chromosomal deletions or rearrangements due to increased repair of double-strand DNA breaks by non-homologous end joining (NHEJ)(11). In this case, suppression can occur through NHEJ inactivation, thereby favoring double-strand break repair by the compromised but more accurate HR machinery (11). Similar trends are observed for genes involved in transcription, for which suppression interactions between pathways mainly represent activation or repression of transcription (Fig. 1D). For example, mutations in genes encoding Mediator or RNA polymerase II subunits can reduce transcription efficiency, which can suppress the toxic effects of derepressed transcription caused by loss-of-function mutations in the NC2 transcription regulator complex (12). Thus, by integrating data from hundreds of papers, we derived a suppression network that provides insight on general suppression relationships and the ordering of pathways and complexes within a biological process.

Suppression interactions within and across cellular processes

Consistent with other biological networks (2, 13–15), many suppression interactions occurred between functionally related genes, such that a query mutant tended to be suppressed by another gene annotated to the same biological process (Fig. 2A). Genes connected by suppression interactions also tended to be co-expressed and encode proteins that function in the same sub-cellular compartment and/or belong to the same pathway or protein complex (Fig. 2B). The extent of functional relatedness between suppression gene pairs did not depend on the conditions under which the interaction was identified (e.g. a specific drug or carbon source), or whether the suppressor was isolated as a spontaneous suppressor mutation as opposed to an engineered allele that was directly tested for an interaction (Fig. S2A). However, the frequency of shared complex membership was significantly higher for gene pairs in which the suppressor gene carried a gain-of-function mutation compared to loss-of-function suppressor mutations ($p=0.01$, Fisher's Exact test). Thus, when a query mutation perturbs a subunit of a complex, compensating mutations in another subunit are more likely to be gain-of-function, for example by stabilizing the complex.

Notably, the functional enrichment observed in the genetic suppression network was substantially stronger than in a global network of negative and positive genetic interactions generated with SGA (6) (Fig. 2B). In fact, most positive genetic interactions identified in the global SGA network, especially among loss-of-function alleles of essential genes, do not overlap with other functional interaction data, highlighting suppression interactions as a special class of positive genetic interaction that captures highly specific functional relationships between gene pairs (Fig. S2B).

Despite their tendency to connect functionally related genes, suppression interactions also connect different biological processes. These interactions often occurred between genes involved in related processes, such as Golgi/endosome/vacuole sorting and ER-Golgi traffic (Fig. 2A). Interestingly, genes involved in protein degradation suppress growth defects associated with mutation of genes involved in many different biological processes. This central role for protein turnover in the suppression network likely reflects a more general mechanism whereby growth defects of conditional temperature sensitive (TS) alleles of essential query genes, which are often hypomorphic (partially functional) even at a permissive temperature, can be overcome by additional mutations that weaken the protein degradation machinery and elevate protein levels.

Overlap with other genetic networks

The suppression network shows significant overlap with a dosage suppression network (13) and with SGA-derived positive and negative genetic interaction networks (2, 6). The overlap with positive genetic interactions (5-fold enrichment; Fig. 2C) is expected, as suppression interactions are an extreme type of positive interaction. Indeed, this overlap increases (11-fold enrichment) for stronger positive genetic interactions. The overlap of the suppression network with dosage suppression interactions associated with gene overexpression reflects that overexpression may lead to a gain-of-function phenotype (16) and suppression can

involve gain-of-function alleles (Figs. 2C, S2C). Gain-of-function suppressor mutations also explain the 2.5-fold enrichment for negative genetic interactions between loss-of-function alleles (Figs. 2C, S2C). For example, whereas the growth defect associated with loss-of-function mutations in *CDC25*, which encodes the guanine nucleotide exchange factor that activates Ras2, can be suppressed by gain-of-function mutations in *RAS2*, loss-of-function mutations in *RAS2* exacerbate the *cdc25* growth defect leading to a synthetic lethal negative genetic interaction (Fig. 2D). Despite the overlap with other genetic networks, most suppression interactions (78%) are specific to the suppression network and thus provide novel insights into the functional wiring diagram of a cell.

Systematic identification of spontaneous suppressor mutations

Literature-curated data can come from specific hypothesis-driven experiments and may thus be biased (15, 17). We therefore compared the curated suppression network to an independent experimental set of spontaneous suppressor mutations identified through the large-scale application of SGA analysis. In SGA, a specific *natMX*-marked query mutation is crossed to an array of ~5000 *kanMX*-marked deletion mutants, to systematically construct a complete set of haploid *natMX*- and *kanMX*-marked double mutants (18, 19). This also represents a genome-wide set of two-factor crosses, enabling us to scan the query strain genome for the presence of an unmarked extragenic suppressor locus, which SGA analysis reveals as a collinear set of small colonies spanning the genomic location of the suppressor mutation, which we refer to as a linkage group (20, 21) (Fig. S3A). In total, we completed 7056 full-genome SGA screens, involving mutant strains carrying deletion or hypomorphic alleles of 5845 different genes (2, 6). In 251 SGA screens (~4%), we identified a linkage group that suggested the presence of a spontaneous extragenic suppressor mutation (Tables S2, S3).

The 251 candidate suppressor strains were analyzed by whole-genome sequencing, and for 216 (86%) of these, a mutation was discovered within the suppressor locus identified by SGA (Fig. S3A, Table S2). Almost all (98%) of these mutations were subsequently confirmed by Sanger sequencing (Table S2). For 24 genes, multiple independently generated query strains carried a potential extragenic suppressor mutation (Table S2). In 13 (54%) of these 24 cases, the extragenic suppressor mutations were in the same gene, while in the remaining 11 cases two different suppressor genes were identified. In three instances, these different suppressor genes encoded known members of the same complex.

We next validated candidate suppressor genes using several genetic tests, including plasmid-based complementation assays, and tetrad analysis of meiotic progeny derived from crossing each suppressor strain to either a wild type strain, a strain with a marked deletion that was genetically linked to the candidate suppressor, or a strain carrying a deletion or hypomorphic allele of the suppressor gene (Fig. S3A) (21). 88% of the suppressor interactions gave a positive result in at least one assay (Table S2). Based on these assays and the type of mutation, one third (33%) of the suppressor mutations appeared to be gain-of-function, while two thirds (67%) appeared to be loss-of-function mutations. We also randomly selected four potential loss-of-function and five potential gain-of-function suppressor alleles and introduced those into a diploid strain that was heterozygous for the corresponding query

mutation. In all cases, sporulation and tetrad analysis of the resulting diploids confirmed the genetic interaction and identity of the suppressor mutation (Table S2, Fig. S3A). Thus, we identified 216 unbiased mutations that arose spontaneously to suppress severe growth defects associated with 146 deletion mutants of nonessential genes and 70 hypomorphic alleles of essential genes (Table S2).

Although we observed significant overlap with the literature-curated dataset (15 shared interactions, $p=1\times 10^{-29}$, Fisher's Exact test), most of the spontaneous suppression interactions identified through SGA (92%) have not been reported previously, indicating that the yeast genetic suppression network has remained largely unexplored. The experimentally-derived suppression interactions showed similar significant enrichments as the literature-curated set for different types of genetic interactions, as well as for functionally related gene pairs, suggesting that suppression interactions in both networks define close functional relationships between genes and share the same basic properties (Fig. S3B, C).

Suppression interaction magnitude correlates with functional relatedness

Given that suppression interactions tend to connect functionally related genes, we examined if the relative magnitude of a given suppression interaction was indicative of the extent of functional overlap. We estimated the relative magnitude of suppression for our systematic interactions (Table S4) (21), ranked the suppression pairs by suppression magnitude and calculated the fraction of functionally related pairs for the 33% strongest and weakest suppression interactions (Fig. S4). Gene pairs exhibiting more severe suppression interactions showed stronger enrichments for various measures of functional relatedness (Fig. S4), in line with what has been described for positive and negative genetic interactions (2). Thus, large improvements in fitness appear to be caused by mutations in genes that are functionally similar to the query, while weaker suppression may be achieved by more general or diverse mechanisms.

Systematic analysis identifies suppressor hubs

The literature-curated network is enriched for genes involved in highly studied processes, such as chromatin and transcription, and DNA replication and repair (Fig. 3A). In contrast, in the experimentally-derived network, queries and suppressors were more evenly spread over the various biological processes. As we found for the literature network (Fig. 2), genes involved in protein degradation were specifically overrepresented as suppressors in the systematic study (Fig. 3A), which mainly reflects suppression of point-mutation alleles of essential queries. Although no significant functional enrichment was found for genes involved in RNA processing, nonsense-mediated mRNA decay genes suppressed several DAMP alleles of essential genes (22), which affect mRNA stability through disruption of their 3' UTR. Thus, restoring protein or mRNA levels may represent a widespread mechanism to overcome growth defects caused by hypomorphic alleles.

Interestingly, suppressed queries with roles in ribosome biogenesis and translation were underrepresented in the literature, but overrepresented in our systematic dataset (Fig. 3A). This enrichment was driven by a set of 34 query genes, each encoding a component of the

mitochondrial translation machinery. Strikingly, all 34 queries were suppressed by missense mutations in the α , β , or γ subunits of the F₁-domain of the mitochondrial ATP synthase, and the majority of the substituted residues were located at the interfaces between these subunits (Fig. 3B). Mutations in the same mitochondrial ATP synthase subunits also suppressed deletion alleles of mitochondrial DNA and RNA polymerase genes, as well as three relatively uncharacterized genes *IRC19*, *PET130*, and *YPR117W* (Table S2). All of these query mutations led to loss of the mitochondrial genome (mtDNA), which results in decreased growth due to a defect in the import of proteins into the mitochondria (23) (Figs. 3C, D, S5A). The ATP synthase suppressor mutations could restore both fitness and mitochondrial protein import in the absence of mtDNA (Figs. 3C, D, S5B). Interestingly, an activity of the ATP synthase other than ATP synthesis was required for this suppression phenotype (Fig S5C, D). Although the mechanism by which the suppressor mutations increase protein import is unclear, one possibility is that the mutations reverse ATP synthase activity to generate ADP³⁻ instead of ATP⁴⁻. The charge difference between these two nucleotide phosphates could be exploited by adenine nucleotide translocators to rebuild the mitochondrial membrane potential, which is lost in the absence of mtDNA, and is thought to be required for protein import into the mitochondria (Fig. 3D) (24).

Suppressor identification can predict novel gene function

The functional relationship observed between a query mutant and its suppressor can be exploited to assign gene function to previously uncharacterized genes. For example, in our systematically mapped suppressor network, we found that loss-of-function mutations in an uncharacterized gene, *YMR010W*, suppressed the growth defect of *mon2* mutants (Fig. 4A, B). Ymr010w belongs to the family of PQ-loop proteins, some of which function as membrane transporters (25), and localizes to both the Golgi and late endosomes (Fig. S6A). Mon2 is distantly related to the Sec7 family of guanine nucleotide exchange factors and physically interacts with Dop1, a conserved membrane protein involved in endosome to Golgi transport, as well as Neo1, an essential member of the phospholipid flippase family (26, 27). When tested directly, we found that a *ymr010w* deletion allele also suppressed the growth defects of *neo1-2* and *dop1-1* TS mutants (Fig. 4B). Moreover, a *ymr010w* deletion allele suppressed the lethality associated with deletion alleles of the essential genes *NEO1* and *DOPI* (Fig. S6B). Loss of *YMR010W* function can thus bypass the requirement for the Mon2/Dop1/Neo1 module.

The essential function of the Mon2/Dop1/Neo1 module is likely performed by Neo1, which is thought to flip phosphatidylserine (PS) and phosphatidylethanolamine (PE) from the exoplasmic to the cytoplasmic leaflet of membrane bilayers, thereby establishing an asymmetric distribution of these lipids (28). A *neo1-2* TS mutant is defective in establishing membrane asymmetry. This leads to hypersensitivity to papuamide A and duramycin, bioactive peptides that disrupt membranes through the binding of exposed PS and PE, respectively (28–30), and reduced plasma membrane localization of GFP-lact-C2, a probe for visualizing the distribution of PS over cytoplasmic membrane leaflets (31) (Fig. 4C, D). Overexpression of *YMR010W* mimicked the phenotype of a *neo1-2* mutant, leading to reduced levels of PS at the cytoplasmic leaflet of the plasma membrane and accumulation of GFP-lact-C2 in internal structures (Fig. 4D). Strikingly, we found that a *ymr010w* deletion

allele suppressed both the sensitivity of a *neo1-2*TS mutant to papuamide A and duramycin (Fig. 4C), and the *neo1-2* GFP-lact-C2 localization defect (Fig. 4D), suggesting that the *neo1-2* phospholipid distribution defects are corrected in the double mutant.

In addition to suppressing loss of Neo1 function, a *ymr010w* deletion allele suppressed the cold sensitivity caused by loss of the flippase Drs2 (Fig. S6C). Moreover, *neo1* lethality was no longer suppressed by *ymr010w* in the absence of Drs2 (Fig. S6C). An intriguing possibility is that Ymr010w functions as a scramblase that transports PS and PE bidirectionally to at least partially collapse the membrane asymmetry established by Neo1 and other flippases (Fig. 4E). Deletion of *YMR010W* would then allow Drs2, possibly with the help of other flippases, to more easily establish membrane asymmetry in the absence of Neo1. We named the *YMR010W* open reading frame *ANY1* for Antagonizes Neo1 Yeast phospholipid flippase.

Frequent secondary mutations delay the onset of stationary phase

Whole-genome sequencing revealed that, besides the suppressor mutation, each suppressor strain carried on average 8 additional secondary mutations (Table S5). Unlike the suppressor mutations, none of these secondary mutations affected exponential cell growth enough to be detected by SGA mapping analysis (Table S3), suggesting the majority are random mutations that arose during DNA replication. We therefore refer to these additional secondary mutations as “passenger” mutations. We identified a similar number of passenger mutations in a control set of 72 strains that did not carry a suppressor mutation that affects growth of the query mutant (Table S5). Of the 304 strains that were sequenced at a coverage >10x, only one query strain, deleted for *PMS1* which encodes a mismatch repair protein, displayed a mutator phenotype, exhibiting a relatively large number (76) of passenger mutations. In total, we identified 2024 unique passenger mutations, of which 996 were in coding regions, affecting 744 protein- or RNA-encoding genes. The fraction of missense, nonsense, and frameshift mutations was significantly smaller among the passenger mutations compared to the suppressor mutations (Fig. 5A). In fact, most of the passenger mutations (64%) resulted in synonymous changes or mapped to intergenic regions (Fig. 5A). Furthermore, passenger missense mutations occurred less frequently in essential genes, were predicted to be less deleterious, were less often at protein-protein interaction interfaces, and occurred more often in disordered protein regions than suppressor missense mutations (Fig. 5B). Thus, the majority of the passenger mutations, which have no effect on exponential growth of the query strain, have a lower putative functional impact than the suppressor mutations that do affect query strain cell growth.

A previous study suggested that deletion of a particular query gene may select for further genetic changes, such as the occurrence of specific secondary non-suppressor mutations (32). However, we did not observe a correlation between the number of passenger mutations and the fitness of the query strain (Fig. S7A). Moreover, genes carrying passenger mutations do not tend to be co-annotated or co-expressed with the corresponding query or suppressor gene (Fig. S7B). In addition, we did not find any significant enrichment for particular GO terms among query genes that shared the same passenger mutation, or for shared passenger mutant genes among multiple, independent isolates of a particular query mutant strain.

However, we found that 10 strains that all carried a suppressor mutation in *ATP2*, but had different query mutations involved in mitochondrial transcription or translation, also harbored a third mutation in *HEM1*, *TPN1*, or *HAP1*. These three genes are important for heme biosynthesis and these mutations may thus be selected for to maintain heme homeostasis in the absence of mitochondrial transcription, translation, or ATP synthase activity. Still, in most cases different isolates of the same query suppressor strains did not contain mutations in the same passenger genes, and most passenger genes were not functionally related to either the query or the suppressor gene, indicating that passenger mutations are not generally dependent on pre-existing mutations.

Interestingly, we did find several genes that were mutated in a large fraction of the sequenced strains, suggesting they may be adaptive and may not represent innocuous passenger mutations (Fig. 5C). Of all sequenced strains, including wild type controls, 29% carried unique mutations in *WHI2*, *IRA1*, *IRA2*, *RIM15*, *CUP9*, and/or *UBC13*. Multiple experimental evolution studies have identified a similar set of frequently mutated yeast genes (33–35). Most of the mutations were frameshift or nonsense mutations, suggesting a selection for loss-of-function of these genes (Fig. 5C). Exponential growth rates of *whi2*, *ira2*, *rim15*, and *ubc13* deletion mutants were not enhanced relative to a *his3* deletion mutant control, suggesting that these frequent secondary mutations were not selected based upon an increased maximum growth rate (Fig. S7C). Strikingly, *Whi2*, *Ira1*, *Ira2*, and *Rim15* are all negative regulators of the RAS/cAMP/PKA pathway which, in response to glucose, stimulates population expansion (36–39). When glucose levels become limited, the RAS/cAMP/PKA pathway is repressed, causing cells to stop dividing and enter stationary phase. Disruptive mutations in *WHI2*, *IRA1*, *IRA2* or *RIM15* may cause a delayed response to low glucose levels, enabling a few additional rounds of cell division prior to entering stationary phase, thereby leading to increased representation of these mutants after serial passaging under laboratory conditions. We constructed mixed populations consisting of a strain deleted for one of the frequently mutated genes and a wild type strain, and followed their ratio for six rounds of serial passaging under conditions with a relatively prolonged stationary phase (21). Indeed, the relative abundance of strains deleted for *WHI2*, *IRA2*, *RIM15*, or *UBC13* increased with each round of serial passaging, whereas five control mutant strains maintained abundances similar to or lower than the wild type reference strain (Figs. 6D, S7D). Similar results were obtained for *IRA1* and *IRA2* in another strain background, W303 (Fig. S7E, F). Thus, our data suggest that the vast majority of passenger mutations are random and not dependent on the query or suppressor mutation, and that a few additional secondary mutations arise at high frequency due to a selection for mutants that delay the onset of the stationary phase.

Mechanistic categories of suppression interactions

We classified the suppression interactions into distinct mechanistic categories on the basis of the functional relationship between query and suppressor. Most queries (54%) reported in the literature or identified by our systematic analysis are suppressed by mutations in functionally related genes (class “A”; Fig. 6A, B). These functional connections can be further divided into four subclasses. Subclass “A1” includes 135 interactions from the literature and systematic networks, in which both the query and the suppressor genes encode

members of the same protein complex. These particular interactions likely reflect a mechanism whereby the suppressor represents a gain-of-function mutation (Fig. S2A). Subclass “A2”, to which 201 interactions from our network were assigned, describes cases where the query mutant growth defect is suppressed by a mutation in a gene that is annotated to the same pathway. In the case of loss-of-function suppressor mutations, the suppressor gene often has antagonistic effects compared to the query gene (e.g. Fig. 4). Subclass “A3” involves suppression by a different, but related, pathway and explains 195 interactions in our networks. In this scenario, the growth phenotype caused by absence of a specific cellular function required for normal cell growth is suppressed when an alternative pathway is rewired to re-create the missing activity (e.g. Fig. 3). Finally, subclass “A4” consists of gene-pairs that are annotated to the same biological process, but for which pathway or complex annotation data was not available for both genes.

In addition to suppression interactions between functionally related genes, suppression interactions involving hypomorphic (partial loss-of-function) alleles - such as conditional TS alleles of essential genes - revealed a different and more general class of suppressors that affect expression of the query gene. This type of suppression (Figs. 2, 3) can be achieved by stabilizing a mutant mRNA or protein through the perturbation of pathways or complexes that regulate mRNA or protein turnover (Fig. 6A, class “B” and “C”). Although this type of suppression is rarely described in the literature, 48% of the hypomorphic queries in our experimental dataset are suppressed by mutations in protein degradation or mRNA decay genes (Fig. 6B), indicating that this type of allele-specific suppression is one of the main routes through which partial loss-of-function alleles can be suppressed. Strikingly, 60–70% of the suppression interactions fall into one of these mechanistic classes, as compared with only 34% of positive genetic interactions identified by SGA (6) and 11% of passenger-query pairs. Thus, positive genetic interactions that are true suppression interactions often show high functional and mechanistic specificity.

Discussion

A global, literature-curated network of genetic suppression interactions (Fig. 1) showed that the majority of suppression interactions linked functionally related genes. Moreover, suppression interactions overlapped significantly with other types of genetic interactions (Fig. 2). Systematic suppression analysis confirmed these general properties of suppression, and further showed that suppression of hypomorphic alleles often occurs via loss of protein or mRNA degradation, a finding that was less obvious in literature-curated data (Fig. 6). The underrepresentation of this class of interactions in the literature is consistent with what has been reported for dosage suppression interactions (13), and may reflect that mechanistic studies focused on the functional analysis of a particular gene or pathway are less likely to report non-specific suppressors. Nevertheless, an understanding of the prevalence of this form of suppression could be important when interpreting a genotype to phenotype relationship. Even though the genes encoding proteasome or mRNA decay components are essential in human cell lines (40–42), we anticipate that genetic variation that subtly modulates the activity of these modules may exhibit genetic interactions associated with a decreased disease risk for a variety of human disorders. As in yeast, these processes may

thus buffer a range of detrimental mutations in humans, and thereby modify numerous different disease phenotypes.

Despite the prevalence of these general suppression mechanisms, most suppression gene pairs showed a close functional relationship (Fig. 6), so that genetic suppression can be used to assign function to a previously uncharacterized gene (Fig. 4). The suppressor interactions identified in our systematic screen resulted from the direct selection of spontaneous mutations during standard laboratory growth of a query mutant whose fitness was compromised. In total, ~3% of strains in the yeast nonessential deletion mutant collection and ~4% of the strains in the hypomorphic essential gene mutant collections showed evidence of a suppressor locus when screened by SGA. Whole genome sequencing of 251 potential suppressor strains did not reveal any instances of suppression via aneuploidy, a mutational event involving copy number variation of many genes, possibly because aneuploidies are not necessarily revealed by SGA genetic mapping, or because these events come at a fitness cost (43). Although SGA suppressor mapping can theoretically identify multiple suppressor mutations within one strain (20), no query strains with multiple suppressor linkages were identified. This suggests that the direct selection for spontaneous suppressors does not mimic adaptive evolution of wild type strains in nutrient-limited conditions, in which aneuploidies and mutations in multiple genes, each contributing small fitness increases, combine to collectively produce a robust suppression phenotype (35, 44). In contrast, we found that there is often a single direct suppression strategy because for most (~67%) of the queries for which we isolated several independent suppressor mutations, these recurrently occurred within the same single suppressor gene or within genes that encode subunits of the same complex. In addition, we found that large increases in fitness are mainly achieved by mutations in genes that have a close functional relation to the query gene (Fig. S4). Thus, only a few, very specific mutational events appear to be able to substantially increase the fitness of a particular query mutant.

Besides the suppressor mutation, each strain also carried on average 8 additional passenger mutations that did not have a measurable effect on exponential growth rate. In a previous but relatively limited study, it was suggested that the deletion of a query gene in the deletion mutant collection often selects for further genetic changes (32). Although this is true for suppressor mutations, we could not find any significant evidence connecting the query or suppressor mutation to the occurrence of most passenger mutations. Because we did not observe a significant enrichment for functionally related gene pairs among queries and passengers, we conclude that the occurrence of query-driven non-suppressor mutations is likely rare.

In a mathematical model of bacterial serial passaging, *de novo* mutations that delay the onset of stationary phase were more likely to fix in a population than mutations that decrease lag time or increase growth or survival rates (45). This may be true for yeast as well, as the growth history of laboratory-grown yeast strains follows a similar pattern of repeating cycles of lag phase, exponential growth, and stationary phase. Indeed, we observe selection for mutations that likely delay the onset of stationary phase in 26% of the sequenced strains (Fig. 5C). These stationary-delay mutations are thus not true 'passenger' mutations, but are adaptive. However, in contrast to suppressor mutations that cause adaptation to the query

mutation, the stationary-delay mutations are adaptive to laboratory passaging. These mutations could come at a cost, as they probably decrease viability during longer periods of starvation (35, 36).

As most (78%) suppression interactions did not overlap with any previously identified genetic interactions, additional suppression mapping will help complete the yeast genetic interaction landscape. Conditional alleles have been developed for nearly all essential yeast genes (6), and thus suppression interactions could be mapped for the full set of essential genes. Similarly, suppressors of nonessential genes could be identified in a conditional or synthetic lethal context in which the nonessential query has a fitness defect. Although we focused on mapping suppression interactions in yeast, similar suppression studies should be possible in mammalian cells and model systems, and may identify new drug targets for query mutations related to human disease (46). As ~6% of human pathogenic variants are fixed in other mammalian species (47), compensatory mutations may be present at a high frequency in natural populations. Understanding genetic suppression may provide insight in how genetic variance accumulates during evolution and more specifically how modifier genes determine the severity of genetic traits, including human disease.

Materials and Methods summary

Detailed materials and methods are available in the supplementary information.

Literature curation

The *Saccharomyces cerevisiae* “synthetic rescue” dataset was downloaded from the BioGRID (9) on November 9, 2012 (version 3.1.49) and on March 31, 2014 (version 3.2.110). In total, these datasets consisted of 5985 interactions described in 1667 papers. Each paper was read in detail, and an interaction was considered a suppression interaction if the double mutant grew significantly better than at least one of the single mutants. For each interaction, suppressor and query allele type and specific conditions were annotated (21). The final dataset consisted of 1842 unique interactions, involving 1304 genes (Table S1).

Systematic suppressor identification

All suppressor strains were part of either the BY4741 nonessential deletion mutant collection (*MATa xxx ::kanMX4 his3 1 leu2 0 ura3 0 met15 0*; Euroscarf), the SGA nonessential deletion mutant collection (*MATa xxx ::natMX4 can1 ::Ste2pr-Sp_his5 lyp1 his3 1 leu2 0 ura3 0 met15 0*; (2)) or the corresponding *MATa* and *MATα* collections of DAmP or TS mutants of essential genes (6). The presence and genomic location of a spontaneous suppressor mutation was identified by the occurrence of a suppressor linkage group upon screening strains in these collections by SGA analysis (20) (Table S3). Potential suppressor strains were subsequently sequenced whole-genome on the Illumina HiSeq 2500 platform using paired-end 100-bp reads. Read mapping and SNP and indel calling was performed using standard methods (21). Candidate suppressor mutations were confirmed by amplifying the corresponding gene and flanking sequences by PCR, followed by Sanger sequencing (Table S2). Suppression interactions were confirmed using plasmid-based complementation assays and tetrad analysis of meiotic progeny derived from

crossing each suppressor strain to either a wild type strain, a strain with a marked deletion that was genetically linked to the candidate suppressor, or a strain carrying a deletion or hypomorphic allele of the suppressor gene (Table S2).

Supplementary Material

Refer to Web version on PubMed Central for supplementary material.

Acknowledgments

We thank G. Fairn, C. Dunn, N. Pascoe, and E. Styles for reagents and technical assistance. This work was primarily supported by grants from the National Institutes of Health (R01HG005853, R01HG005084, P50HG004233 and U01HG001715)(C.B., B.J.A., C.L.M., F.P.R.) the Canadian Institutes of Health Research (FDN-143264 and FDN-143265)(C.B., B.J.A.), and the Ontario Research Fund (Research Excellence Grant) (F.P.R.), the Canada Excellence Research Chairs Program (F.P.R.), and a postdoctoral fellowship from the Canadian Institutes of Health Research (J.v.L.). Additional support was provided by the Canadian Institutes of Health Research (FDN-143301)(A.C.G.), the Vienna Science and Technology Fund (LS08-QM03)(C.O., M.P.), and the National Institutes of Health (R01GM107978)(T.R.G.). C.B., B.J.A., F.P.R., and C.L.M. are Senior Fellows in the Canadian Institute for Advanced Research Genetic Networks program. All whole-genome sequencing data is publicly available at NCBI's Sequencing Read Archive, under accession number SRP067030. All suppression interaction data is included in Tables S1 and S2.

References and Notes

- Dixon SJ, Costanzo M, Baryshnikova A, Andrews B, Boone C. Systematic mapping of genetic interaction networks. *Annu Rev Genet.* 2009; 43:601–625. [PubMed: 19712041]
- Costanzo M, et al. The genetic landscape of a cell. *Science.* 2010; 327:425–431. [PubMed: 20093466]
- Chen R, et al. Analysis of 589,306 genomes identifies individuals resilient to severe Mendelian childhood diseases. *Nat Biotechnol.* 2016; 34:531–538. [PubMed: 27065010]
- St Onge RP, et al. Systematic pathway analysis using high-resolution fitness profiling of combinatorial gene deletions. *Nat Genet.* 2007; 39:199–206. [PubMed: 17206143]
- Breslow DK, et al. A comprehensive strategy enabling high-resolution functional analysis of the yeast genome. *Nat Methods.* 2008; 5:711–718. [PubMed: 18622397]
- Costanzo M, et al. A global genetic interaction network maps a wiring diagram of cellular function. *Science.* 2016 in press.
- Baryshnikova A, et al. Quantitative analysis of fitness and genetic interactions in yeast on a genome scale. *Nat Methods.* 2010; 7:1017–1024. [PubMed: 21076421]
- Botstein, D. *Decoding the language of genetics.* Cold Spring Harbor Laboratory Press; Cold Spring Harbor, New York: 2015.
- Stark C, et al. BioGRID: a general repository for interaction datasets. *Nucleic Acids Res.* 2006; 34:D535–539. [PubMed: 16381927]
- Shannon P, et al. Cytoscape: a software environment for integrated models of biomolecular interaction networks. *Genome Res.* 2003; 13:2498–2504. [PubMed: 14597658]
- Valencia-Burton M, et al. Different mating-type-regulated genes affect the DNA repair defects of *Saccharomyces* RAD51, RAD52 and RAD55 mutants. *Genetics.* 2006; 174:41–55. [PubMed: 16782999]
- Peiro-Chova L, Estruch F. Specific defects in different transcription complexes compensate for the requirement of the negative cofactor 2 repressor in *Saccharomyces cerevisiae*. *Genetics.* 2007; 176:125–138. [PubMed: 17339209]
- Magtanong L, et al. Dosage suppression genetic interaction networks enhance functional wiring diagrams of the cell. *Nat Biotechnol.* 2011; 29:505–511. [PubMed: 21572441]
- Huttlin EL, et al. The BioPlex Network: A Systematic Exploration of the Human Interactome. *Cell.* 2015; 162:425–440. [PubMed: 26186194]

15. Rolland T, et al. A proteome-scale map of the human interactome network. *Cell*. 2014; 159:1212–1226. [PubMed: 25416956]
16. Sopko R, et al. Mapping pathways and phenotypes by systematic gene overexpression. *Mol Cell*. 2006; 21:319–330. [PubMed: 16455487]
17. Cusick ME, et al. Literature-curated protein interaction datasets. *Nat Methods*. 2009; 6:39–46. [PubMed: 19116613]
18. Tong AH, et al. Systematic genetic analysis with ordered arrays of yeast deletion mutants. *Science*. 2001; 294:2364–2368. [PubMed: 11743205]
19. Tong AH, et al. Global mapping of the yeast genetic interaction network. *Science*. 2004; 303:808–813. [PubMed: 14764870]
20. Jorgensen P, et al. High-resolution genetic mapping with ordered arrays of *Saccharomyces cerevisiae* deletion mutants. *Genetics*. 2002; 162:1091–1099. [PubMed: 12454058]
21. Detailed materials and methods are available as supplementary materials at the Science website.
22. Schuldiner M, et al. Exploration of the function and organization of the yeast early secretory pathway through an epistatic miniarray profile. *Cell*. 2005; 123:507–519. [PubMed: 16269340]
23. Dunn CD, Jensen RE. Suppression of a defect in mitochondrial protein import identifies cytosolic proteins required for viability of yeast cells lacking mitochondrial DNA. *Genetics*. 2003; 165:35–45. [PubMed: 14504216]
24. Clark-Walker GD. Kinetic properties of F1-ATPase influence the ability of yeasts to grow in anoxia or absence of mtDNA. *Mitochondrion*. 2003; 2:257–265. [PubMed: 16120326]
25. Jezegou A, et al. Heptahelical protein PQLC2 is a lysosomal cationic amino acid exporter underlying the action of cysteamine in cystinosis therapy. *Proc Natl Acad Sci U S A*. 2012; 109:E3434–3443. [PubMed: 23169667]
26. Gillingham AK, Whyte JR, Panic B, Munro S. Mon2, a relative of large Arf exchange factors, recruits Dop1 to the Golgi apparatus. *J Biol Chem*. 2006; 281:2273–2280. [PubMed: 16301316]
27. Barbosa S, Pratte D, Schwarz H, Pipkorn R, Singer-Kruger B. Oligomeric Dop1p is part of the endosomal Neo1p-Ysl2p-Arl1p membrane remodeling complex. *Traffic*. 2010; 11:1092–1106. [PubMed: 20477991]
28. Takar M, Wu Y, Graham TR. The Essential Neo1 Protein from Budding Yeast Plays a Role in Establishing Aminophospholipid Asymmetry of the Plasma Membrane. *J Biol Chem*. 2016; 291:15727–15739. [PubMed: 27235400]
29. Parsons AB, et al. Exploring the mode-of-action of bioactive compounds by chemical-genetic profiling in yeast. *Cell*. 2006; 126:611–625. [PubMed: 16901791]
30. Iwamoto K, et al. Curvature-dependent recognition of ethanolamine phospholipids by duramycin and cinnamycin. *Biophys J*. 2007; 93:1608–1619. [PubMed: 17483159]
31. Fairn GD, Hermansson M, Somerharju P, Grinstein S. Phosphatidylserine is polarized and required for proper Cdc42 localization and for development of cell polarity. *Nat Cell Biol*. 2011; 13:1424–1430. [PubMed: 21964439]
32. Teng X, et al. Genome-wide consequences of deleting any single gene. *Mol Cell*. 2013; 52:485–494. [PubMed: 24211263]
33. Lang GI, et al. Pervasive genetic hitchhiking and clonal interference in forty evolving yeast populations. *Nature*. 2013; 500:571–574. [PubMed: 23873039]
34. Kryazhimskiy S, Rice DP, Jerison ER, Desai MM. Global epistasis makes adaptation predictable despite sequence-level stochasticity. *Science*. 2014; 344:1519–1522. [PubMed: 24970088]
35. Kvitek DJ, Sherlock G. Whole genome, whole population sequencing reveals that loss of signaling networks is the major adaptive strategy in a constant environment. *PLoS Genet*. 2013; 9:e1003972. [PubMed: 24278038]
36. Cameroni E, Hulo N, Roosen J, Winderickx J, De Virgilio C. The novel yeast PAS kinase Rim15 orchestrates G0-associated antioxidant defense mechanisms. *Cell Cycle*. 2004; 3:462–468. [PubMed: 15300954]
37. Smith A, Ward MP, Garrett S. Yeast PKA represses Msn2p/Msn4p-dependent gene expression to regulate growth, stress response and glycogen accumulation. *EMBO J*. 1998; 17:3556–3564. [PubMed: 9649426]

38. Kaida D, Yashiroda H, Toh-e A, Kikuchi Y. Yeast Whi2 and Psr1-phosphatase form a complex and regulate STRE-mediated gene expression. *Genes cells*. 2002; 7:543–552. [PubMed: 12090248]
39. Tanaka K, et al. *S.cerevisiae* genes IRA1 and IRA2 encode proteins that may be functionally equivalent to mammalian ras GTPase activating protein. *Cell*. 1990; 60:803–807. [PubMed: 2178777]
40. Hart T, et al. High-Resolution CRISPR Screens Reveal Fitness Genes and Genotype-Specific Cancer Liabilities. *Cell*. 2015; 163:1515–1526. [PubMed: 26627737]
41. Wang T, et al. Identification and characterization of essential genes in the human genome. *Science*. 2015; 350:1096–1101. [PubMed: 26472758]
42. Blomen VA, et al. Gene essentiality and synthetic lethality in haploid human cells. *Science*. 2015; 350:1092–1096. [PubMed: 26472760]
43. Torres EM, et al. Effects of aneuploidy on cellular physiology and cell division in haploid yeast. *Science*. 2007; 317:916–924. [PubMed: 17702937]
44. Sunshine AB, et al. The fitness consequences of aneuploidy are driven by condition-dependent gene effects. *PLoS Biol*. 2015; 13:e1002155. [PubMed: 26011532]
45. Wahl LM, Zhu AD. Survival probability of beneficial mutations in bacterial batch culture. *Genetics*. 2015; 200:309–320. [PubMed: 25758382]
46. Buchovecky CM, et al. A suppressor screen in Mecp2 mutant mice implicates cholesterol metabolism in Rett syndrome. *Nat Genet*. 2013; 45:1013–1020. [PubMed: 23892605]
47. Jordan DM, et al. Identification of cis-suppression of human disease mutations by comparative genomics. *Nature*. 2015; 524:225–229. [PubMed: 26123021]
48. Huttenhower C, Hibbs M, Myers C, Troyanskaya OG. A scalable method for integration and functional analysis of multiple microarray datasets. *Bioinformatics*. 2006; 22:2890–2897. [PubMed: 17005538]
49. Huh WK, et al. Global analysis of protein localization in budding yeast. *Nature*. 2003; 425:686–691. [PubMed: 14562095]
50. Kanehisa M, Sato Y, Kawashima M, Furumichi M, Tanabe M. KEGG as a reference resource for gene and protein annotation. *Nucleic Acids Res*. 2016; 44:D457–462. [PubMed: 26476454]
51. Hu Y, et al. Approaching a complete repository of sequence-verified protein-encoding clones for *Saccharomyces cerevisiae*. *Genome Res*. 2007; 17:536–543. [PubMed: 17322287]
52. Kainth P, et al. Comprehensive genetic analysis of transcription factor pathways using a dual reporter gene system in budding yeast. *Methods*. 2009; 48:258–264. [PubMed: 19269327]
53. Li H, Durbin R. Fast and accurate short read alignment with Burrows-Wheeler transform. *Bioinformatics*. 2009; 25:1754–1760. [PubMed: 19451168]
54. Li H, et al. The Sequence Alignment/Map format and SAMtools. *Bioinformatics*. 2009; 25:2078–2079. [PubMed: 19505943]
55. Ye K, Schulz MH, Long Q, Apweiler R, Ning Z. Pindel: a pattern growth approach to detect break points of large deletions and medium sized insertions from paired-end short reads. *Bioinformatics*. 2009; 25:2865–2871. [PubMed: 19561018]
56. Vaser R, Adusumalli S, Leng SN, Sikic M, Ng PC. SIFT missense predictions for genomes. *Nat Protoc*. 2016; 11:1–9. [PubMed: 26633127]
57. Mosca R, Ceol A, Aloy P. Interactome3D: adding structural details to protein networks. *Nat Methods*. 2013; 10:47–53. [PubMed: 23399932]
58. Peng K, Radivojac P, Vucetic S, Dunker AK, Obradovic Z. Length-dependent prediction of protein intrinsic disorder. *BMC bioinformatics*. 2006; 7:208. [PubMed: 16618368]
59. Oates ME, et al. D(2)P(2): database of disordered protein predictions. *Nucleic Acids Res*. 2013; 41:D508–516. [PubMed: 23203878]
60. Kabaleeswaran V, Puri N, Walker JE, Leslie AG, Mueller DM. Novel features of the rotary catalytic mechanism revealed in the structure of yeast F1 ATPase. *EMBO J*. 2006; 25:5433–5442. [PubMed: 17082766]
61. Kall L, Krogh A, Sonnhammer EL. A combined transmembrane topology and signal peptide prediction method. *J Mol Biol*. 2004; 338:1027–1036. [PubMed: 15111065]

62. Kim H, Melen K, Osterberg M, von Heijne G. A global topology map of the *Saccharomyces cerevisiae* membrane proteome. *Proc Natl Acad Sci U S A*. 2006; 103:11142–11147. [PubMed: 16847258]

Author Manuscript

Author Manuscript

Author Manuscript

Author Manuscript

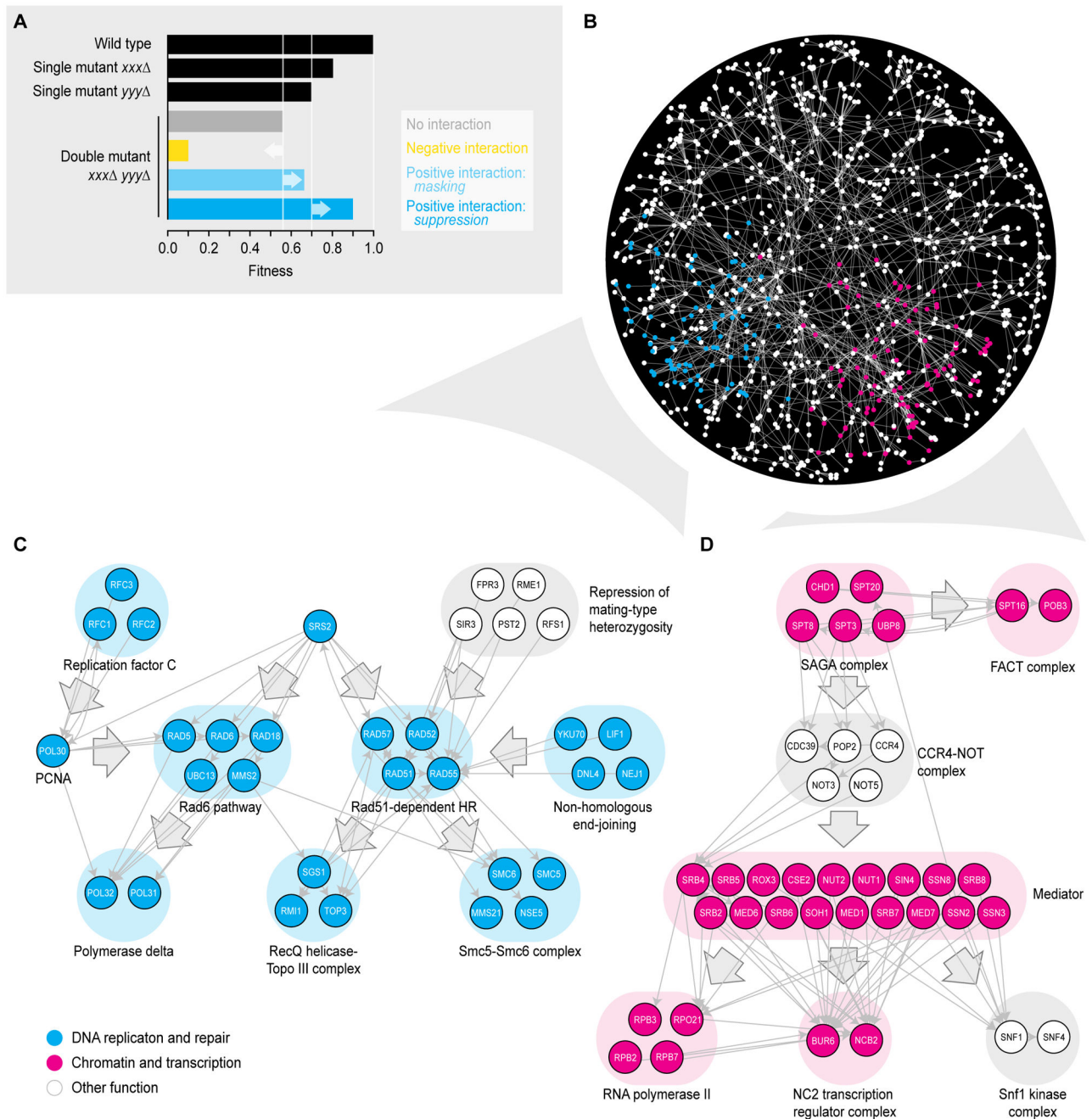


Fig. 1. A global network of literature-curated suppression interactions for *S. cerevisiae*. (A) Genetic interaction classes. When two single mutants (*xxx* and *yyy*) have a relative fitness of 0.8 and 0.7, the expected fitness of the resultant double mutant (*xxx yyy*) based on a multiplicative model is $0.8 \times 0.7 = 0.56$. A negative genetic interaction occurs when the observed double mutant fitness is lower than this expected fitness. A masking positive interaction occurs when the fitness of the double mutant is greater than expected, but lower or equal to that of the slowest growing single mutant. Suppression positive interactions occur when the double mutant fitness is greater than that of the slowest growing single mutant. (B)

A global network of literature-curated suppression interactions for *S. cerevisiae*. Genes are represented as nodes and interactions as edges. The nodes were distributed using a force-directed layout, such that genes that share a suppressor tend to be close together on the network. Genes involved in chromatin and transcription or DNA replication and repair are highlighted in magenta and cyan, respectively. **(C,D)** Regions of the global network highlighting suppression interactions between complexes and pathways involved in chromatin and transcription (C) or DNA replication and repair (D) are shown. Arrows point from the suppressor to the query.

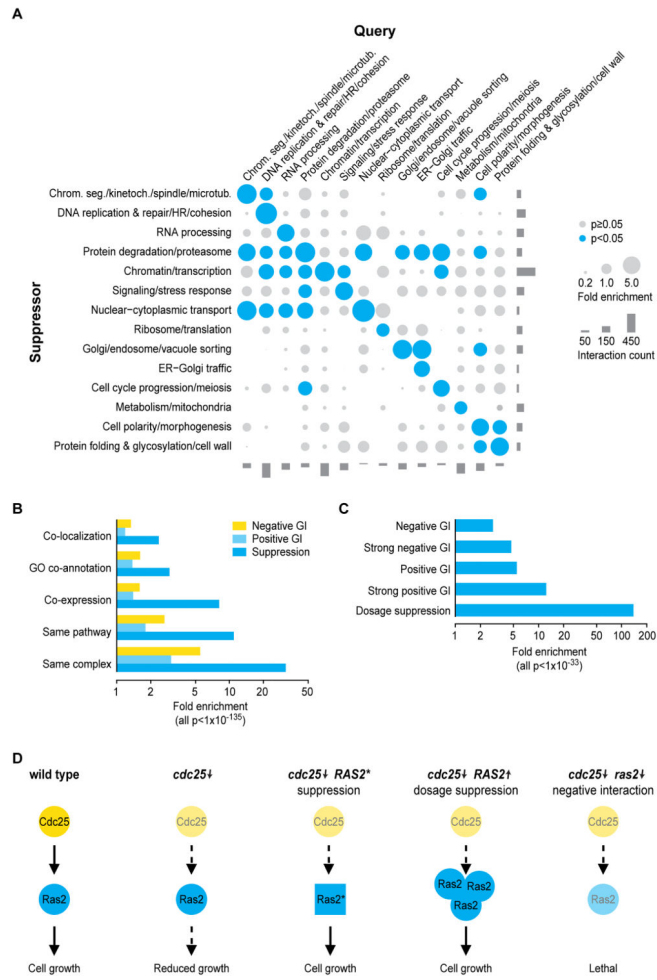


Fig. 2. Properties of the suppression network

(A) Frequency of suppression interactions connecting genes within and across indicated biological processes. Node size reflects fold enrichment for interacting gene pairs observed for a given pair of biological processes. Significance of the enrichment was determined by Fisher’s Exact test, comparing the observed frequency of suppression interactions between two given functional categories with the global frequency. The total number of suppression interactions involving genes annotated to a particular process is indicated. (B,C) Fold enrichment for: (B) co-localization, GO co-annotation, co-expression, same pathway membership, and same complex membership for gene pairs involved in different types of genetic interaction (GI); and (C) overlap of literature-curated suppression interactions with dosage suppression interactions (13), or with negative and positive genetic interactions identified by SGA analysis using either an intermediate or a stringent interaction score threshold (6). A Fisher’s Exact test was performed to determine statistical significance of the results. (D) An example of a gene pair showing suppression, dosage suppression, and negative genetic interactions.

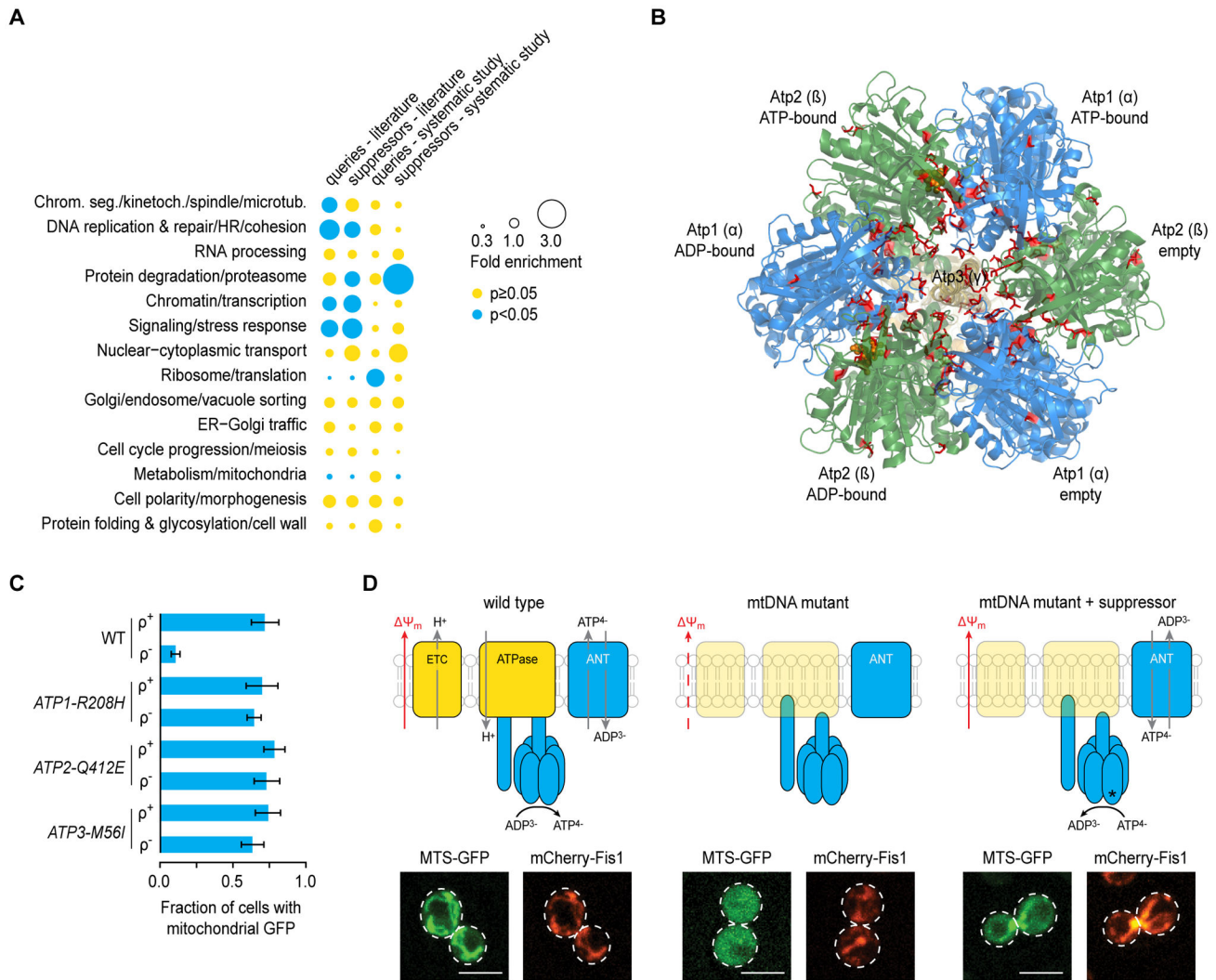


Fig. 3. The mitochondrial F₁-ATPase is a suppressor hub in the systematic suppression network (A) The distribution of query and suppressor mutants in both the literature-curated and the systematic experimental network across different biological processes. Node size reflects fold enrichment or depletion for query and suppressor mutants observed for a given biological processes. Significant enrichment or depletion was determined by Fisher’s Exact test, comparing the observed to the expected proportion of genes in each functional category. Bonferroni-corrected p-values are indicated. (B) Bottom-view, facing the inner-membrane from the mitochondrial matrix, of the yeast mitochondrial F₁-ATPase structure 2HLD. Residues that were found to suppress the growth defect of mitochondrial transcription or translation mutants are highlighted in red. Orange spheres represent the nucleotides bound to the catalytic sites. (C) Fraction of wild type and ATP synthase-mutant cells either with intact (ρ⁺) or (partially) deleted (ρ⁻) mtDNA that show mitochondrial localization of GFP fused to a mitochondrial-targeting signal (MTS-GFP). Averages (n=4) and SD are shown. (D) Model of ATP synthase-dependent suppression of mitochondrial mutants (top) and corresponding representative images of MTS-GFP import (bottom). Localization of outer-mitochondrial membrane protein mCherry-Fis1 shows the presence and position of mitochondria.

Abbreviations: ETC, electron transport chain; Ψ_m , inner mitochondrial membrane potential; ANT, adenine nucleotide translocator. Scale bar: 5 μ m.

Author Manuscript

Author Manuscript

Author Manuscript

Author Manuscript

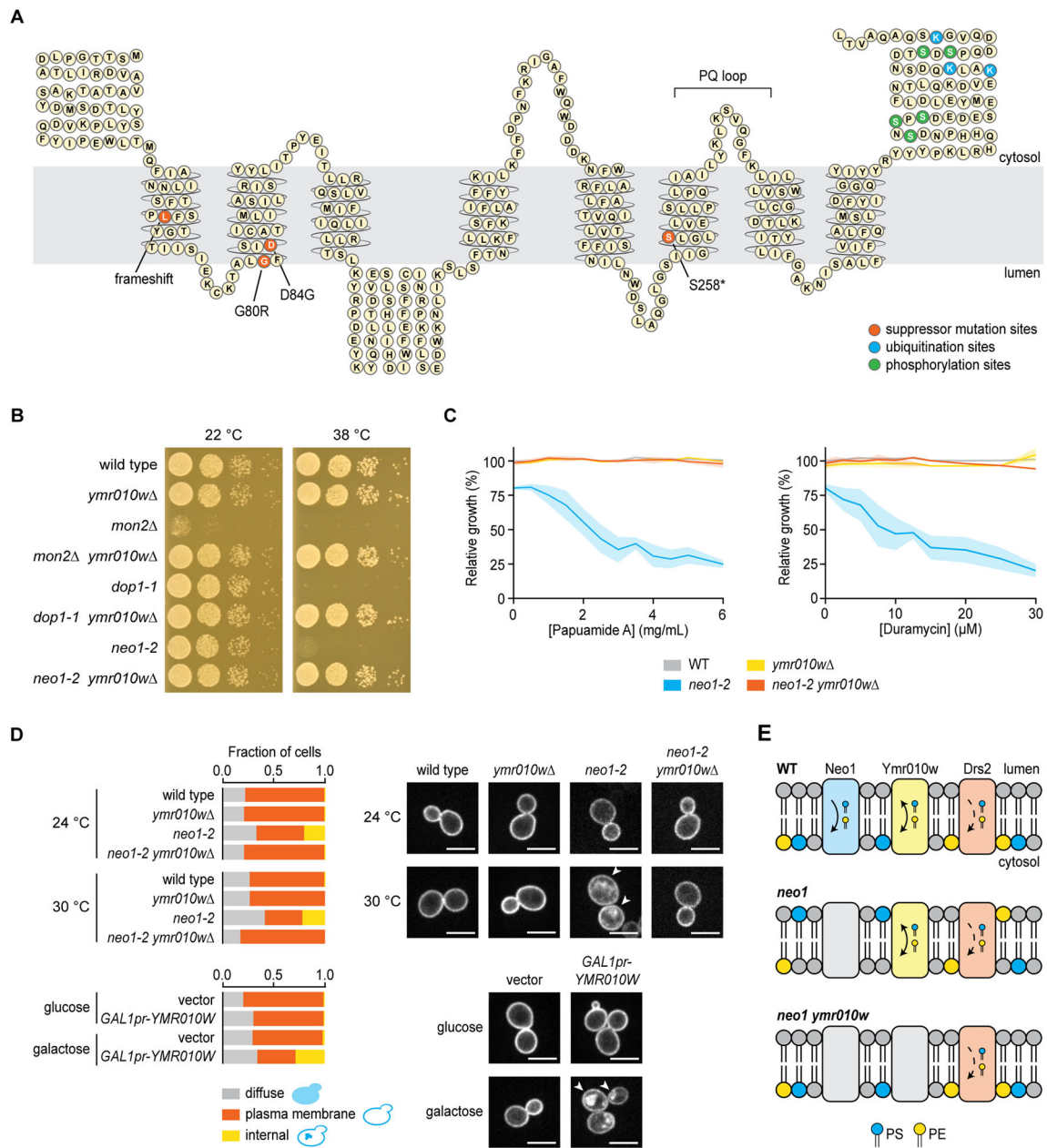


Fig. 4. Characterization of YMR010W (ANY1)

(A) Predicted membrane topology of Ymr010w. Sites of suppressor mutations, ubiquitination and phosphorylation are indicated. (B) Suppression of the growth defect caused by a *mon2* deletion allele, or TS alleles *dop1-1* and *neo1-2*, by deletion of YMR010W. Series of ten-fold dilutions of exponentially growing cultures of the indicated strains were spotted on YPD plates and incubated at either 22°C or 38°C for 2 days. (C) Deletion of YMR010W restores membrane asymmetry in *neo1-2* cells. Wild type, *ymr010w*, *neo1-2* and *neo1-2 ymr010w* cells were grown at 34°C in the presence of the phosphatidylserine (PS) targeting peptide papuamide A or the phosphatidylethanolamine (PE) targeting peptide duramycin. Growth relative to vehicle-treated wild type strain is

plotted. SEM is indicated by shading ($n=2-3$). **(D)** Intracellular distribution of PS, visualized using GFP-lact-C2 (31). Shown are representative confocal fluorescent micrographs of exponentially growing cells using the indicated strains. The fraction of cells that showed diffuse cytosolic fluorescence, localization of GFP-lact-C2 to the plasma membrane, or in which GFP-lact-C2 was partially localized to distinct internal structures, was calculated. Measurements were performed in triplicate on at least 100 cells, and averages are shown. **(E)** Model of suppression of flippase mutants by loss of Ymr010w.

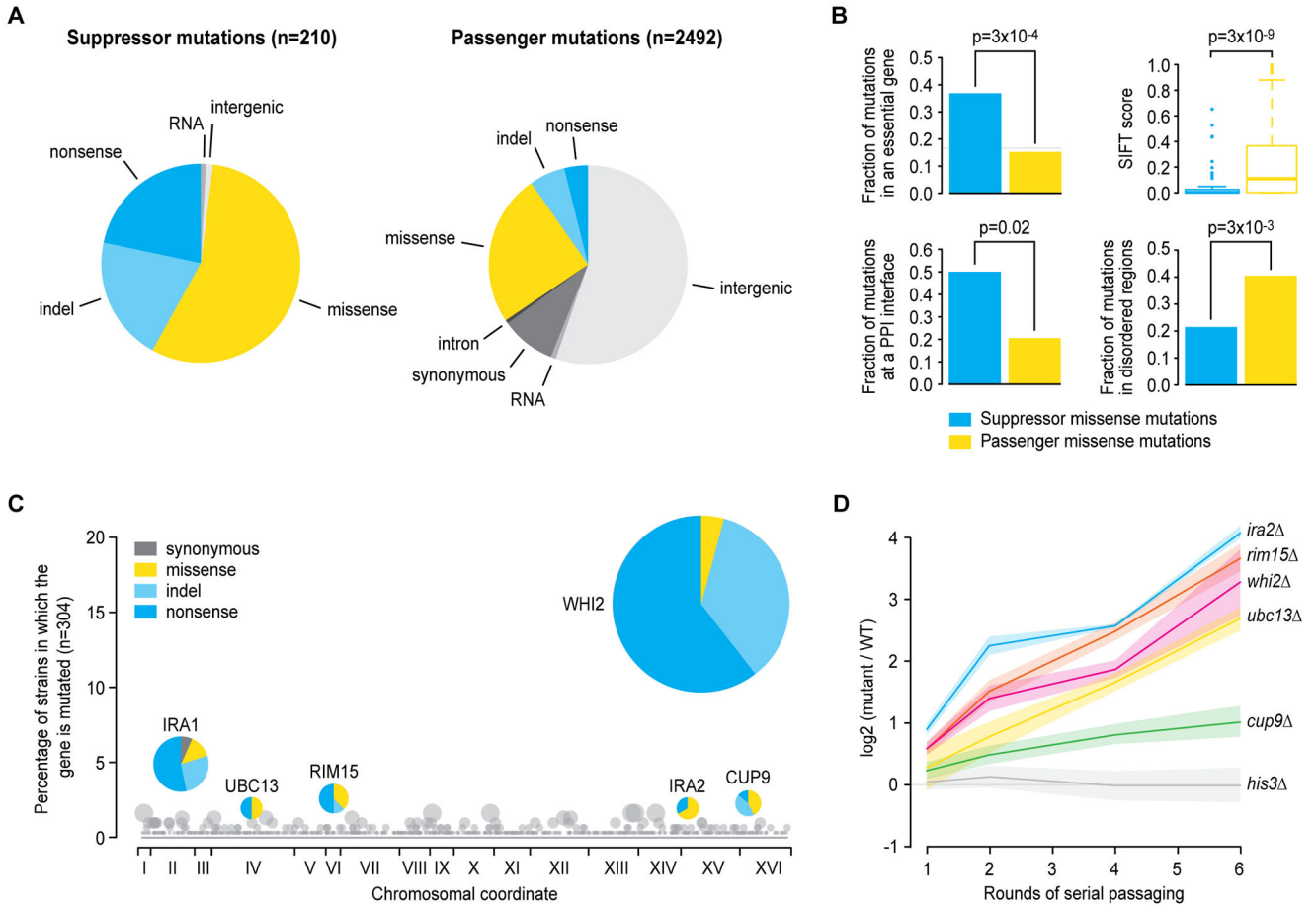


Fig. 5. Characterization of potential passenger mutations

(A) Distribution of suppressor and potential passenger mutations over variant effect classes. Only SNPs are considered, as reliable structural variant calls (deletions, insertions, or inversions involving >5 basepairs) were only available for suppressor mutations. The RNA class refers to mutations in an RNA species such as a non-coding, ribosomal, or transfer RNA. (B) The fraction of all suppressor or potential passenger missense mutations that map to an essential gene, at a protein-protein interaction (PPI) interface, or a disordered region of a protein, and the predicted deleteriousness of these mutations (SIFT score 0 = extremely deleterious, 1 = benign). P-values were calculated using Fisher’s Exact test, except for the SIFT analysis, in which a Mann-Whitney’s test was used. (C) The percentage of strains in which a particular gene carries a passenger mutation is plotted against the chromosomal position of the gene. Genes that are recurrently mutated in >2% of the sequenced strains are highlighted, and the distribution of the mutations over variant effect classes is shown. (D) Differentially fluorescently labeled cells of the indicated mutants (RFP) and wild type (GFP) were mixed, and the ratio of RFP to GFP was followed for 6 rounds of serial passaging on agar plates. Shading represents the SD, n=12.

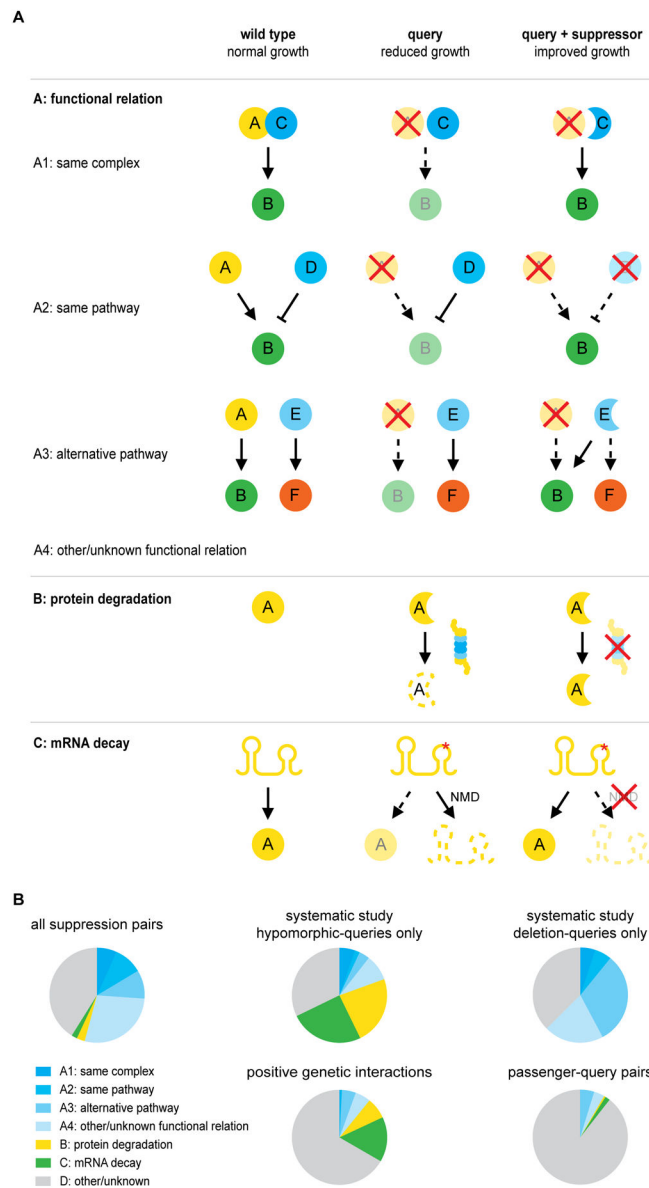


Fig. 6. Mechanistic classes of suppression

(A) Suppressor and query genes often have a functional relationship (class “A”). In a situation where the query (protein A) activates a protein B, which is required for normal growth, suppression can take place in multiple ways. For example, the suppressor (protein C) can be part of the same complex as the query, and gain-of-function mutations in C can restore the activation of B (class “A1”). Alternatively, the suppressor and query may be members of the same pathway, and the suppressor (protein D) may inactivate or inhibit B. Loss of D may thus suppress by partially restoring the activity of B (class “A2”). The suppressor (protein E) can also function in an alternative, but related, pathway, whose activity can be slightly altered to restore the activity of B (class “A3”). Suppression interactions can also occur among pairs of genes that do not share a close functional relationship. For example, partial loss-of-function query alleles may carry mutations that

destabilize the protein or mRNA, leading to a fitness defect caused by reduced levels of the query protein. This can be suppressed by a loss-of-function mutation in a member of the protein degradation (class “B”) or mRNA decay (class “C”) pathway, which may partially restore the levels of the query protein. **(B)** Distribution of suppression interactions, positive genetic interactions (6), and passenger-query pairs across different mechanistic suppression classes.